Dynamic Modeling and Resilience for Power Distribution

Yun Wei and Chuanyi Ji
School of Electrical and Computer Engineering
Georgia Institute of Technology
Atlanta, Georgia 30332–0250
Email: yunwei@gatech.edu
jichuanyi@gatech.edu

Floyd Galvan, Stephen Couvillon and George Orellana
Entergy Services, Inc.
New Orleans, LA 70053
Email: fgalvan@entergy.com
scouvi1@entergy.com
gorella@entergy.com

***Abstract*—Resilience of power distribution is pertinent to the energy grid under severe weather. This work develops an analytical formulation for large-scale failure and recovery of power distribution induced by severe weather. A focus is on incorporating pertinent characteristics of topological network structures into spatial temporal modeling. Such characteristics are new notations as dynamic failure- and recovery-neighborhoods. The neighborhoods quantify correlated failures and recoveries due to topology and types of components in power distribution. The resulting model is a multi-scale non-stationary spatial temporal random process. Dynamic resilience is then defined based on the model. Using the model and large-scale real data from Hurricane Ike, unique characteristics are identified: The failures follow the 80/20 rule where 74.3% of the total failures result from 20.7% of failure neighborhoods with up to 72 components "failed" together. Thus the hurricane caused a large number of correlated failures. Unlike the failures, the recoveries follow 60/90 rule: 59.3% of recoveries resulted from 92.7% of all neighborhoods where either one component alone or two together recovered. Thus about 60% recoveries were uncorrelated and required individual restorations. The failure and recovery processes are further studied through the resilience metric to identify the least resilient regions and time durations.**

I. Introduction

A key objective of the smart grid is to improve resilience of the power grid to external disruptions from severe weather. Severe weather events such as hurricanes and storms have been occurring more frequently in America in recent years, each of which resulted in a half to several million customers without electricity for days [1] [2]. Power distribution was often impacted the most, as a compound effect of severe weather and an out-dated infrastructure. Distribution networks lie at the edge of the grid with a large number of components across a wide geographical span. Those components can be either aging or not well-protected, and are thus susceptible to severe weather.

A fundamental research issue pertaining to this real problem is the resilience of power distribution to large-scale external disruptions from severe weather [3]. Resilience here corresponds to the ability of the grid to withstand external disturbances and to recover rapidly from failures [4].

Empirical approaches have been used widely in industry for weather induced failures [5]. However, empirical approaches become inadequate for large-scale weather-induced disruptions that occur frequently in recent years [2]. Static models are developed for identifying variables related to failures of power distribution [6] [7] [8]. However, dynamic models and resilience are needed for characterizing the time-varying nature of weather-induced large-scale failure and recovery [9].

Resilience involves multiple spatial-temporal scales. A small spatial scale is at the component-level where failures and restorations occur. A large spatial scale is at the subnetwork-level where resilience is measured through aggregating component failures and recoveries in a service area. A small temporal scale of subminutes is when topologically correlated failures occur [10], and when electricity is regained through self-healing [11]. A large temporal scale of minutes and beyond is when failures and restorations occur due to severe weather and manual repair respectively. For resilience to encompass the pertinent multi-scale characteristics, a rigorous problem formulation is necessary from bottom-up, i.e., from modeling to defining resilience/vulnerability at the multiple scales. This work develops such an approach by focusing on the following challenges.

The first challenge is stochasticity where failures and recoveries occur randomly and dynamically. Failure stochasticity results from spatial-temporal evolution of external weather [9]. Recovery stochasticity results from environmental conditions of the aftermath of a severe weather event. In addition, failures and restorations exhibit non-stationarity, i.e., different behaviours at different time and locations [9]. Existing approaches in power systems account for randomness of failures [12] [13] [5] but rarely the dynamics nor spatial-temporal non-stationarity. In our prior work, a spatial-temporal non-stationary stochastic model is developed at the large spatial scale of cities and temporal scale of minutes [9]. However, network structures of power distributions are not considered. A recent work [14] provides a rigorous formulation for the minimum number of PMU monitors in distribution networks, and motivates our formulation.

This work includes the effect of network structures through a new notion of dynamic neighborhoods. Dynamic neighborhoods characterize how weather-induced failures are exacerbated by a network structures. The resulting model is a spatial-temporal non-stationary random process that encompasses

topological network structures, different network components, dynamic failure and recovery.

The second challenge is how to define resilience. Static metrics on resilience have been widely used [15]. These metrics, however, do not characterize the dynamic nature of large-scale failures induced by severe weather. In addition, resilience needs to include recovery from failures [16]. This work defines the resilience as a dynamic metric, motivated by those from communication networks [17]. Importantly, the dynamic resilience metric is based on the spatial temporal model derived from bottom up. The metric thus reflects the impact of dynamic network neighborhoods in addition to weather-induced failures and recoveries.

The non-stationary model and the resilience metric are applied to a real life example of large scale power failures during Hurricane Ike in 2008. Real data from an operational network is used to learn parameters of failure and recovery processes as well as the resilience metric. This results in insights and understanding on the resilience of operational networks in Section V.

II. Problem Setting

A. Problem Description

Consider a node that represents a network component such as a substation, a transformer, or a link as a feeder/power line. Severe weather can induce a failure directly to a node. For example, flooding can cause a non-functional substation and other equipment failures. High winds can cause fallen poles or trees on power lines. Such weather-induced failures often occur in minutes resulting from evolving severe-weather conditions [9].

A weather-induced failure, referred to as a failure in short, can result in secondary failures through a network structure. A network structure consists of a topology and different types of components. For example, unbalanced currents from a failure can cause burned line fuses as secondary failures. A failure upstream can also result in losses of electricity, but no damage, at nodes downstream in a distribution tree. For example, either a non-functional substation or a broken link cause a loss of power to downstream nodes. Those nodes without electricity service are referred to as outages. Secondary failures and outages occur at a smaller time scale of subminutes, as impacted by a network structure. Disruptions include failures, secondary failures and outages.

Recovery occurs at two time-scales also. Self-recovery occurs in subminutes. Manual repairs to damaged nodes occur at the time scale of minutes or longer [9]. When a failure- or an outage-node regains electricity supply, downstream outage nodes regain the service together. Hence, the multi-scale characteristics need to be quantified for disruption and recovery respectively.

B. Failure and Neighborhoods

Let $X_i^{(w)}(t)$ be the state of node i at time t, where i specifies both a network location and a geo-location of the node, $1 \leq i \leq n$. n is the total number of nodes in a network. $t > 0$ is continuous time. For simplicity, a node takes two states: $X_i^{(w)}(t) = 1$ if node i is in disruption. $X_i^{(w)}(t) = 0$ if node i is in normal operation. w specifies three scenarios: $w = f$ for a failure induced by exogenous weather, $w = f'$ for a secondary failure, and $w = o$ for an outage. An outage or a secondary failure is induced by a failure occurred at a network neighbor. A network neighbor here is a node at the upstream of a distribution network with a tree topology.

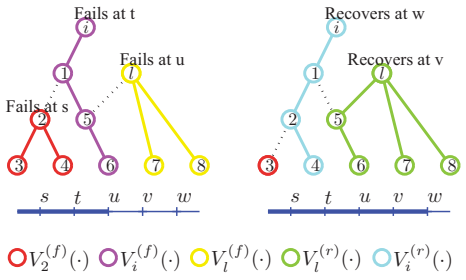

Fig. 1. Example of neighborhoods.

Disruption $A_i^{(w)}(t)$ is a state transition from normal to disruption $\{X_i^{(w)}(t - \Delta t) = 0, X_i^{(w)}(t) = 1\}$, which occurs in $(t - \Delta t, t]$ at node i, $t > 0$, $w = \{f, f', o\}$. $\Delta t > 0$ is sufficiently small so that there is only one failure, and one set of secondary failures or outages occurred in $(t - \Delta t, t]$.

Failure neighborhood $V_i^{(f)}(t)$ is a new notion of dynamic topology, consisting of the downstream nodes that are in normal operation preceding failure i at $t - \Delta t$. That is, for any $j \in V_i^{(f)}(t)$, either outage $A_j^{(o)}(t)$ or secondary failure $A_j^{(f')}(t)$ occur with failure i. Hence, a failure neighborhood characterizes correlated failures and outages.

C. Recovery and Neighborhoods

Recovery $B_i^{(w)}(t)$ is the state transition from disruption to normal $\{X_j^{(w)}(t - \Delta t) = 1, X_j^{(w)}(t) = 0\}$, which occurs in $(t - \Delta t, t]$ at node i, $t > 0$, $w = \{f, f', o\}$. When $w = f$ (or $w = f'$), failure i is repaired. When $w = o$, an upstream neighbor of node i is repaired.

Recovery neighborhood $V_i^{(r)}(t)$ is another new notion of dynamic topology, consisting of the downstream neighbors of node i that are in outage at $(t - \Delta t, t)$ prior to the restoration. $\Delta t > 0$ is sufficiently small so that there is one restoration and one set $V_i^{(r)}(t)$ of recoveries in $(t - \Delta t, t]$.

D. Example

Figure 1 shows an example of disruption and recovery as well as the neighborhoods. First, node 2 fails at time s, inducing secondary failure 3 and outage 4, i.e., $V_2^{(f)}(s) = \{3, 4\}$. Then node i fails at $t > s$, inducing outages to nodes in failure neighborhood $V_i^{(f)}(t) = \{1, 5, 6\}$. Then node l fails at $u > t$, inducing outages to $V_l^{(f)}(u) = \{7, 8\}$. Note that

node 5 is a downstream neighbor of both nodes i and l but only belongs to failure neighborhood $V_i^{(f)}(t)$ of node i by definition. Hence failure neighborhoods are non-overlapping for failures occurred at different locations and time.

Failure l is repaired at $v > u$, restoring failure l and outages in recovery neighborhood $V_l^{(r)}(v) = \{5, 6, 7, 8\}$. Finally, failure i is repaired at $w > v$, restoring failure i and outages in $V_i^{(r)}(v) = \{1, 2, 4\}$. Secondary failure 3 remains to be restored. This example illustrates failure- and recovery-neighborhoods that are dynamically changing due to evolving failures and reconfiguration in restoration.

III. Non-Stationary Spatial Temporal Processes

A dynamic network environment emerges from the above problem setting: External severe weather causes network nodes to fail. The failed nodes induce secondary failures and outages at their network neighbors. Failures/outages then recover together with their neighbors. Such disruption and recovery are modeled as non-stationary spatial temporal random processes, with dynamic neighborhoods at the component-level, and aggregations of components in a service region.

A. Disruption Process

Our modeling starts from the component-level. n nodes in a tree topology form a spatial temporal process, consisting of a network of random state transitions as binary variables $\{I[A_i^{(w)}(t)], I[B_i^{(w)}(t)]\}$, for $t > 0, 1 \leq i \leq n, w = \{f, f', o\}$. $I(A)$ is an indicator function. $I(A) = 1$ if the event A occurs; otherwise, $I(A) = 0$. Let $\Delta N_i^{(d)}(t)$ be the number of nodes that are disrupted from electricity service in $(t - \Delta t, t]$. For a sufficiently small $\Delta t > 0$, it is natural to assume that only one weather-induced failure occurs at node i, and one set of related secondary failures and outages in $(t - \Delta t, t]$. Then

$$\Delta N_i^{(d)}(t) = I[A_i^{(f)}(t)] + v_i^{(f)}(t) I[A_i^{(f)}(t)], \tag{1}$$

where $v_i^{(f)}(t) I[A_i^{(f)}(t)]$ is a set of secondary failures and outages in neighborhood $V_i^{(f)}(t)$. $v_i^{(f)}(t) = ||V_i^{(f)}(t)||$ is the size of the failure neighborhood at node i and time t. $v_i^{(f)}(t)$ characterizes correlated disruptions. The larger $v_i^{(f)}(t)$ is, the more correlated disruptions for the node at time t.

Definition *1:* **Failure, outage and disruption rate**. Failure rate of node i at time t is the expected number of state transitions from normal to (weather-induced) failures per unit time at node i, which is

$$\lambda_i^{(f)}(t) = \lim_{\Delta t \to 0} \frac{E\left\{I[A_i^{(f)}(t)]\right\}}{\Delta t}. \tag{2}$$

Here $E\{\cdot\}$ represents expectation. Outage rate that is induced by failure i at time t is the expected number of state transitions from normal to outage per unit time at failure neighborhood $V_i^{(f)}(t)$. For simplicity of notation, the outage rate here includes secondary failures also, where

$$\lambda_i^{(o)}(t) = \lim_{\Delta t \to 0} \frac{E\left\{v_i^{(f)}(t) I[A_i^{(f)}(t)]\right\}}{\Delta t}. \tag{3}$$

Disruption rate at node i is $\lambda_i^{(d)}(t) = \lim_{\Delta t \to 0} \frac{1}{\Delta t} E\{\Delta N_i^{(d)}(t)\}$,

$$\lambda_i^{(d)}(t) = \lambda_i^{(f)}(t) + \lambda_i^{(o)}(t). \tag{4}$$

A disruption rate shows the impact of severe weather and a network structure. A failure neighborhood shows explicitly impacts of topology and heterogeneous types of components.

B. Recovery Process

The number of nodes that are recovered in $(t - \Delta t, t]$ can be obtained similarly,

$$\Delta N_i^{(r)}(t) = I[B_i^{(f)}(t)] + v_i^{(r)}(t) I[B_i^{(f)}(t)], \tag{5}$$

where $I[B_i^{(f)}(t)]$ is the state of recovery for failure i. $v_i^{(r)}(t) = ||V_i^{(r)}(t)||$ is the size of a recovery neighborhood $V_i^{(r)}(t)$. Recovery process is characterized by the recovery rate defined as follows.

Definition *2:* **Recovery rate**. The recovery rate for node i and its neighbors in $V_i^{(r)}(t)$ at time t is

$$\lambda_i^{(r)}(t) = \lim_{\Delta t \to 0} \frac{E\left\{I[B_i^{(f)}(t)](1 + v_i^{(r)}(t))\right\}}{\Delta t}. \tag{6}$$

The recovery rate and neighborhoods are dynamic, showing a changing topology in restoration. The time-varying rates and neighborhoods show the non-stationarity of disruption- and recovery-processes.

C. Aggregation at Subnetwork-Level

Now let $N^{(w)}(t)$ be the number of disruptions in a subnetwork in a service region,

$$E\{N^{(w)}(t)\} = \int_0^t \lambda_{i(\tau)}^{(w)}(\tau) d\tau, \tag{7}$$

where $w = \{f, f', o\}$. $i(\tau)$ indicates the location of a disruption i at time τ. $d\tau$ is assumed to be small so that at most one failure and one neighborhood of secondary failures/outages occur in $(\tau - d\tau, \tau)$. The expected number of disruptions $E\{N^{(d)}(t)\}$ occurred up to time t is the sum of expected failures and outages (with secondary failures),

$$E\{N^{(d)}(t)\} = E\{N^{(f)}(t)\} + E\{N^{(o)}(t)\}. \tag{8}$$

Let $E\{N^{(r)}(t)\}$ be the expected number of nodes which recover in $[0, t]$ in a subnetwork, then

$$E\{N^{(r)}(t)\} = \int_0^t \lambda_{i(\tau)}^{(r)}(\tau) d\tau. \tag{9}$$

IV. Resilience

The non-stationary spatial temporal model enables a novel resilience metric for power distribution. Before the metric is defined, we first characterize fast versus slow recovery based on concepts from infant and aging mortality [18].

Definition *3:* Infant (fast) and aging (slow) recovery: Let $d_0 > 0$ be a threshold value. If a node remains in either

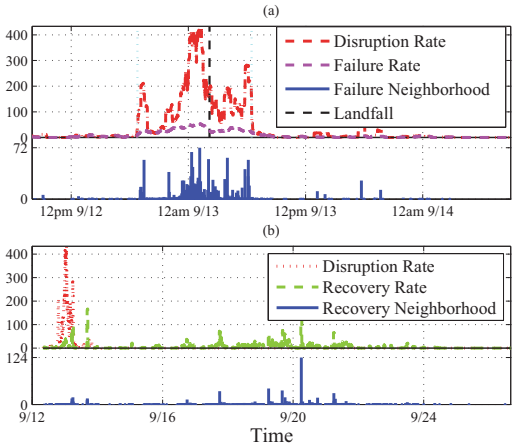

Fig. 2. Empirical rate functions of the network: (a) Failure rate, disruption rate, and size of failure neighborhood; (b) Recovery rate and size of recovery neighborhood.

failure or outage for less than d_0 duration, the node has infant recovery. Otherwise, the node has aging recovery.

Using threshold d_0, we can define resilience. Intuitively, resilience measures network-wide performance from two aspects. One is for a power grid to withstand external disruptions as much as possible. The other is to rapidly restore electricity service from failures. Hence, aging recovery is a complement of these two characteristics [9]. Resilience is then characterized as one minus aging recovery.

Definition *4:* **Resilience**: Consider a sub-network in region Z with m number of disruptions. The resilience of the subnetwork is,

$$s(t,Z) = 1 - \frac{1}{m}\int_{\tau=0}^{t}\left(\sum_{w=f,o}\sum_{i(\tau)\in Z}\lambda_{i(\tau)}^{(w)}(\tau) \Pr\{D_{i(\tau)}^{(w)}(\tau) > t-\tau+d_0\}\right)d\tau. \quad (10)$$

The second term corresponds to the expected percentage of aging recoveries at time t. The aging recoveries here correspond to disruptions at time t that would not recover for at least additional duration d_0. For example, when $w = f$, $\lambda_{i(\tau)}^{(f)}d\tau$ is the expected number of disruptions occurred in $(\tau - d\tau, \tau]$. $\Pr\{D_{i(\tau)}^{(w)}(\tau) > t-\tau+d_0\}$ is the probability for failures to last a duration longer than $t-\tau+d_0$. The product is the expected number of nodes that fail in $(\tau - d\tau, \tau]$ and do not recover at time $t+d_0$, which is simply the number of aging recoveries viewed at time t. The integral adds up all aging recoveries in duration $[0,t]$ and region Z. Hence, $s(t,Z)$ is the expected percentage of nodes in region Z at time t which are either in normal operation or recover within additional duration d_0. The resilience thus reflects temporal evolution of a network in response to severe weather.

V. Hurricane Ike and Large-Scale Real Data

The non-stationary spatial temporal model is now applied to studying the impact of a major hurricane. Real data from an operational network is used to obtain empirical disruption and recovery rates and to understand impacts of network structures.

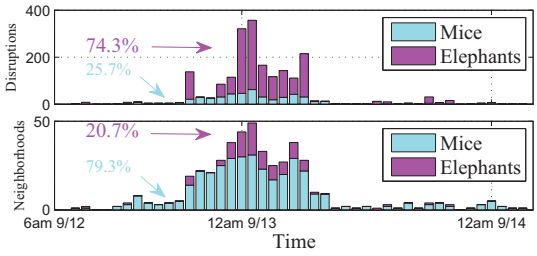

Fig. 3. Histogram of the disruptions and failure neighborhoods over time. Size of elephants neighborhoods is more than 2.

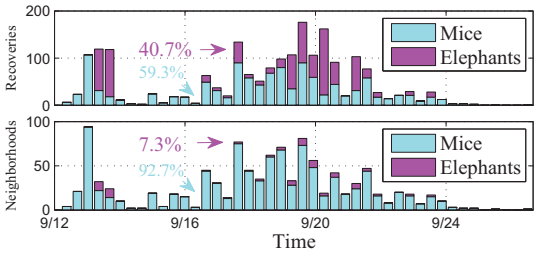

Fig. 4. Histogram of the recoveries and recovery neighborhoods over time. Size of elephants neighborhoods is more than 2.

A. Real Data and Processing

Hurricane Ike is one of the strongest hurricanes that occurred in 2008. Ike resulted in more than two million customers without electricity in Louisiana and Texas [19]. A major utility provider collected data on component failures and outages. Our data set consists of 2004 samples (failures or outages) that occurred from 7 a.m. September 12th to 4 a.m. September 14th, during which Hurricane Ike made the landfall. Each sample consists of occurrence time, duration and location (latitude and longitude) of a disruption for a component in a distribution network. The accuracy for time t is one minute.

A failure neighborhood includes samples whose failure/ outage occurrences fall within a minute. There are 204 failure neighborhoods of sizes $1 \sim 72$. The remaining 260 failures occurred individually with minutes apart. Similarly, samples with recovery occurrences within a minute are in a recovery neighborhood. There are 241 recovery neighborhoods and 824 individual recoveries.

B. Empirical Non-Stationary Processes

We now study the empirical non-stationary processes, the impact of topological network structures, and the resilience using the real data.

1) Empirical Disruption Process: We estimate empirical failure rate $\hat{\lambda}^{(f)}(t)$ and disruption rate $\hat{\lambda}^{(d)}(t)$ by aggregating over the components. The disruption rate takes into account of failure neighborhoods. The failure rate is calculated by aggregating disruptions occurred in a minute as one "failure".

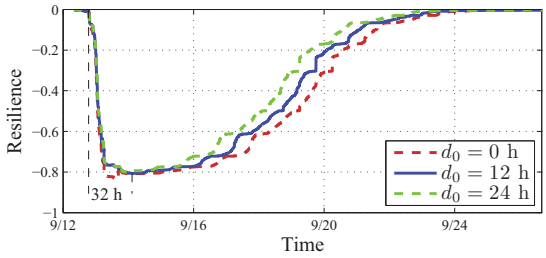

Fig. 5. Resilience of the entire power distribution.

A simple moving average is used [20], where $\hat{\lambda}^{(w)}(t) = \frac{1}{2\tau}\left(\hat{N}^{(w)}(t+\tau) - \hat{N}^{(w)}(t-\tau)\right)$, with $\tau = 1$ hour, $w = \{d, f\}$. Figure 2(a) shows the disruption and failure rates respectively.

The rates and the failure neighborhoods are time-varying, showing the non-stationarity of the disruption process. The failure rate increased to the peak value of 50 new failures per hour around the landfall. The disruption rate exhibited a similar behavior but had a larger peak value of 450 new disruptions per hour around the landfall.

The much larger disruption rate reflects the impact of dynamic network structure: There were a large number of correlated disruptions during the hurricane. This is further shown in Figure 2(a) where large failure neighborhoods occurred mainly during the intense hurricane period, with as many as 72 disruptions in one neighborhood. Hence, the network components and topology were impacted by the hurricane differently during its evolution.

2) Empirical Recovery Process: Recovery rate $\hat{\lambda}^{(r)}(t)$ and the size of recovery neighborhood $v_{i(t)}^{(r)}(t)$ are estimated similarly and shown in Figure 2(b). Two bursts of recoveries emerge. The first is infant recovery that occurred along with major failures within six hours after the landfall. The second is aging recovery that occurred about 7.7 hours after. The recovery rate and the size of the recovery-neighborhoods vary with time, showing the non-stationarity of the recovery process.

C. Neighborhoods: Impact of Network Structures

Dynamic failure neighborhoods are indicative of the impacts of topological network structures and the hurricane. The large failure neighborhoods around the landfall shown in Figure 2(a) indicate that the hurricane induced a large number of correlated disruptions. In contrast, failures that occurred individually happened mainly before and after the hurricane. This suggests that correlated failures/outages occurred at the small time scale of subminutes is a pertinent characteristic of the hurricane-induced disruptions.

Using the analogy of elephant and mice flows in computer communication [21], we refer large neighborhoods as elephants, and small neighborhoods as mice. An 80/20 rule emerges for the disruption process: Elephants failure neighborhoods of size more than 2 contribute to 74.3% of total disruptions as shown in Figure 3. However, the elephants failure neighborhoods amount to only 20.7% of the total failure neighborhoods. This implies that the majority of disruptions are correlated and induced by elephant failures.

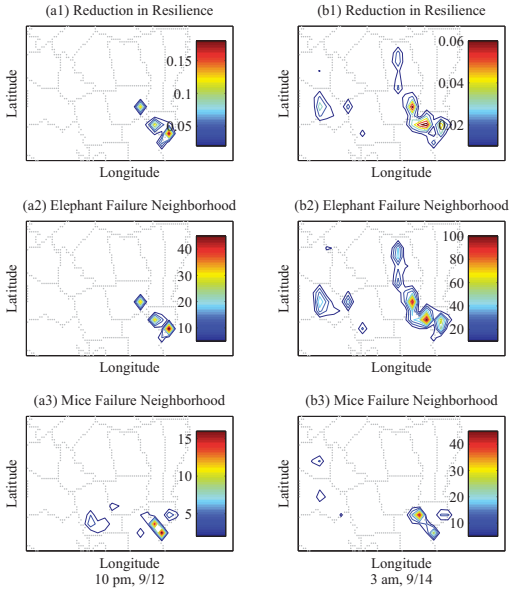

Fig. 6. Two snapshots of the resilience over the geographical area of the power distributions: (a) Reduction in percentage (of total number of disruptions) for resilience; (b) Number of neighborhoods for elephants failures; (c) Number of neighborhoods for mice failures.

Unlike the disruptions, recovery neighborhoods follow the 60/90 rule: The mice recovery neighborhoods of size 2 or less take up 92.7% of all recovery neighborhoods, amounting to 59.3% of recoveries, as shown in Figure 4. This suggests that around 60% recoveries were uncorrelated, and thus required individual restorations.

D. Resilience: Identifying Vulnerability

We now obtain the empirical resilience in terms of aging recovery using real data.

1) Vulnerable Time: In general, threshold d_0 can be determined through failure and recovery rates (see [9] for details). Here in Figure 2(b), the empirical recovery rate clearly shows that infant recovery occurred along with the majority of the failures, and is for the failures that lasted less than 12 hours. After the infant recovery, there is a delay of 7.7 hours before aging recovery occurred. Therefore, the threshold is $d_0 = 12$ hours.

The resilience is calculated using $d_0 = 12$ in Equation 10. As shown in Figure 5, the resilience decreased from the normal operations along with the failure occurrences, and reached a maximum reduction of 80.7% of total disruptions. The time at the minimum resilience is 32 hours since the initial failure occurrence. This was the most vulnerable time when the infant recovery already ended and the aging recovery was yet to begin. The minimum resilience indicates that 80.7% of total

disruptions needed at least another $d_0 = 12$ hours to recover. This is consistent to the resilience curve that it took up to 14 days for all disruptions to recover.

What if threshold d_0 is chosen differently? If $d_0 = 0$ is chosen, the infant recovery would be incorrectly considered as a part of non-resilience. The resulting resilience is thus overly pessimistic with a maximum reduction of 83.7% rather than 80.7% in Figure 5. On the other hand, if $d_0 = 24$ is chosen, the threshold falsely excludes parts of aging recovery, resulting in overly optimistic resilience. Hence, identifying an optimal threshold is important and shall be considered in the future work.

2) Vulnerable Areas: The resilience metric can also be used to identify vulnerable areas in a service region. Figure 6(a1) and (b1) show the percentage reduction of the resilience at two time epoches: 4 hours before the landfall and the time of the minimum resilience. The regions with more than 15% and 6% reduction of resilience appear as vulnerable areas for the two time epoches. Figure 6(a2) and (b2) show the number of elephant failure neighborhoods at the two times respectively. The vulnerable areas coincide with the regions that have a large number of elephant failure neighborhoods. This is consistent with the finding in Section V-C that elephant failure neighborhoods contribute to the majority of the disruptions and thus a significant deduction of the resilience. Mice failure neighborhoods, however, are not coupled with the vulnerable areas. These findings pose interesting directions for more detailed study at the component level.

VI. Conclusion

This work develops a spatial-temporal non-stationary random process to model large-scale disruptions of power distribution induced by severe weather. The model combines non-stationary failure- and recovery-random processes with network structures. Dynamic failure- and recovery-neighborhoods are defined to characterize a topological network structure. The neighborhoods characterize correlated failures and recoveries within networks. Dynamic disruption- and recovery-rates are used as simple quantities for failure- and recovery processes at both component- and subnetwork-level. A resilience metric resulting from the model then characterizes the evolution of failure and recovery. Real data from an operational network during Hurricane Ike is used to study the resilience and the impact of dynamic neighborhoods. An 80/20 rule emerges for failures, showing that hurricane-induced power-disruptions are mostly correlated due to network structures. In contrast, recoveries occur mainly in small patches, and thus required individual restorations. These findings reveal disparities between large-scale failures and recoveries processes, suggesting more in-depth studies at the component level for identifying vulnerabilities and improving resilience.

References

[1] H. Rudnick, "Natural Disasters Their Impact on Electricity Supply," *IEEE Power and Energy Magazine*, vol. 9, no. 2, pp. 22–26, March/April 2011, 2011.

[2] W. N. Bryan, "Emergency Situation Reports: Hurricane Sandy," Office of Electricity Delivery and Energy Reliability of U.S. Department of Energy, Hurricane Sandy Situation Report 20, November 2012.

[3] G. A. Pagani and M. Aiello, "The Power Grid as a Complex Network: A Survey," *Physica A: Statistical Mechanics and its Applications*, vol. 392, no. 11, pp. 2688–2700, 2013.

[4] Y. Wei, C. Ji, F. Galvan, S. Couvillon, G. Orellana, and J. Momoh, "Non-Stationary Random Process for Large-Scale Failure and Recovery of Power Distributions," *arXiv.org*, vol. abs/1202.4720, 2012.

[5] D. Zhu, "Electric Distribution Reliability Analysis Considering Time-Varying Load, Weather Conditions and Reconfiguration with Distributed Generation," Ph.D. dissertation, Virginia Polytechnic Institute and State University, 2007.

[6] P. J. Maliszewski and C. Perrings, "Factors in the Resilience of Electrical Power Distribution Infrastructures," *Applied Geography*, vol. 32, no. 2, pp. 668–679, 2012.

[7] R. Nateghi, S. D. Guikema, and S. M. Quiring, "Comparison and Validation of Statistical Methods for Predicting Power Outage Durations in the Event of Hurricanes," *Risk Analysis*, vol. 31, no. 12, pp. 1897–1906, December 2011.

[8] C. Rudin, D. Waltz, R. Anderson, A. Boulanger, A. Salleb-Aouissi, M. Chow, H. Dutta, P. Gross, B. Huang, and S. Ierome, "Machine Learning for the New York City Power Grid," *IEEE Trans. Pattern Anal. Mach. Intell.*, vol. 34, no. 2, pp. 328–345, Feb. 2012.

[9] Y. Wei, C. Ji, F. Galvan, S. Couvillon, G. Orellana, and J. Momoh, "Learning Geotemporal Non-Stationary Failure and Recovery of Power Distribution," 2013, to appear in *Special Issue of Non-Stationary and Evolutionary Learning, IEEE Trans. on Neural Networks and Learning Systems*.

[10] H. Xiao and E. Yeh, "Cascading Link Failure in the Power Grid: A Percolation-Based Analysis," in *Communications Workshops (ICC), 2011 IEEE International Conference on*, 2011, pp. 1–6.

[11] M. Amin and J. Stringer, "The Electric Power Grid: Today and Tomorrow," *MRS Bulletin*, vol. 33, pp. 399–407, Apr. 2008.

[12] P. Hines, J. Apt, and S. Talukdar, "Large Blackouts in North America: Historical Trends and Policy Implications," *Energy Policy*, vol. 37, no. 12, pp. 5249–5259, December 2009.

[13] I. Dobson, B. Carreras, and D. Newman, "A Branching Process Approximation to Cascading Load-Dependent System Failure," in *37th Hawaii International Conference on System Sciences*, Hawaii, Jan 2004.

[14] Y. Zhao, R. Sevlian, R. Rajagopal, A. Goldsmith, and H. V. Poor, "Outage Detection in Power Distribution Networks with Optimally-Deployed Power Flow Sensors," in *Proceedings of the 2013 IEEE Power and Energy Society General Meeting*, Vancouver, BC, Canada, July 2013.

[15] J. P. G. Sterbenz, D. Hutchison, E. K. Çetinkaya, A. Jabbar, J. P. Rohrer, M. Schöller, and P. Smith, "Resilience and Survivability in Communication Networks: Strategies, Principles, and Survey of Disciplines," *Comput. Netw.*, vol. 54, no. 8, pp. 1245–1265, June 2010.

[16] R. J. Ellison, D. A. Fisher, R. C. Linger, and et al, "Survivable Network System: An Emerging Discipline," Software Engineering Institute, Carnegie Mellon University, Pittsburgh, PA, Technical Report CMU/SEI-97-TR-013, November 1997.

[17] K. S. Trivedi, D. S. Kim, and R. Ghosh, "Resilience in Computer Systems and Networks," in *Proceedings of the 2009 International Conference on Computer-Aided Design*, ser. ICCAD '09. New York, NY, USA: ACM, 2009, pp. 74–77.

[18] J. D. Kalbfleisch and R. L. Prentice, *The Statistical Analysis of Failure Time Data*, 2nd ed. New York: John Wiley and Sons, 2002.

[19] J. Colley and S. M. DeBlasio Sr, "Hurricane Ike Impact Report," U.S. Department of Homeland Security, Technical Report, December 2008.

[20] H. L. V. Trees, *Detection, Estimation, and Modulation Theory*. New York: Wiley, 1971, vol. 1.

[21] K. C. Lan and J. Heidemann, "A Measurement Study of Correlation of Internet Flow Characteristics," *Computer Networks*, vol. 50, no. 1, pp. 46–62, January 2006.